AIDS RESEARCH AND HUMAN RETROVIRUSES
Volume 30, Number 6, 2014

DOI: 10.1089/aid.2013.0182

Modulation of Gut-Specific Mechanisms by Chronic Δ^9-Tetrahydrocannabinol Administration in Male Rhesus Macaques Infected with Simian Immunodeficiency Virus: A Systems Biology Analysis

Patricia E. Molina, Angela M. Amedee, Nicole J. LeCapitaine, Jovanny Zabaleta, Mahesh Mohan, Peter J. Winsauer, Curtis Vande Stouwe, Robin R. McGoey, Matthew W. Auten, Lynn LaMotte, Lawrance C. Chandra, and Leslie L. Birke

Abstract

Our studies have demonstrated that chronic Δ^9-tetrahydrocannabinol (THC) administration results in a generalized attenuation of viral load and tissue inflammation in simian immunodeficiency virus (SIV)-infected male rhesus macaques. Gut-associated lymphoid tissue is an important site for HIV replication and inflammation that can impact disease progression. We used a systems approach to examine the duodenal immune environment in 4- to 6-year-old male rhesus monkeys inoculated intravenously with SIV_{MAC251} after 17 months of chronic THC administration (0.18–0.32 mg/kg, intramuscularly, twice daily). Duodenal tissue samples excised from chronic THC- ($N=4$) and vehicle (VEH)-treated ($N=4$) subjects at $\sim$5 months postinoculation showed lower viral load, increased duodenal integrin beta 7^+($\beta7$) $CD4^+$ and $CD8^+$ central memory T cells, and a significant preferential increase in Th2 cytokine expression. Gene array analysis identified six genes that were differentially expressed in intestinal samples of the THC/SIV animals when compared to those differentially expressed between VEH/SIV and uninfected controls. These genes were identified as having significant participation in (1) apoptosis, (2) cell survival, proliferation, and morphogenesis, and (3) energy and substrate metabolic processes. Additional analysis comparing the duodenal gene expression in THC/SIV vs. VEH/SIV animals identified 93 differentially expressed genes that participate in processes involved in muscle contraction, protein folding, cytoskeleton remodeling, cell adhesion, and cell signaling. Immunohistochemical staining showed attenuated apoptosis in epithelial crypt cells of THC/SIV subjects. Our results indicate that chronic THC administration modulated duodenal T cell populations, favored a pro-Th2 cytokine balance, and decreased intestinal apoptosis. These findings reveal novel mechanisms that may potentially contribute to cannabinoid-mediated disease modulation.

Introduction

Cannabinoids are one of the most commonly used and abused drugs.[1] The major psychoactive cannabinoid in marijuana, Δ^9-tetrahydrocannabinol (THC), exerts unique effects on the progression of simian immunodeficiency virus (SIV) infection. Previous studies from our laboratory have shown that chronic THC administration ameliorates SIV disease progression and significantly reduces the morbidity and mortality of male SIV-infected macaques.[2,3] Several organ systems are affected by cannabinoids, including the gastrointestinal tract, the immune system, and the central nervous system. Furthermore, THC can affect numerous cell signaling and effector mechanisms that contribute to the overall systemic response to infection and disease progression, including viral entry into host cells, integration into the host genome, viral replication, and tissue inflammation.[3]

Recent studies have identified the gut-associated lymphoid tissue (GALT) as an important target for HIV and SIV infection.[4] The early depletion of gut $CD4^+$ T cells following infection and their subsequent restoration following initiation of antiretroviral therapy have been demonstrated in serial jejunal biopsies.[5] Moreover, individuals with controlled viral disease, or nonprogressors, show better maintenance of

Departments of Physiology, Pharmacology, and Medicine, and Alcohol and Drug Abuse Center of Excellence, Louisiana State University Health Sciences Center, New Orleans, Louisiana.

GALT CD4$^+$ T cells during the course of HIV infection.[6] Others have suggested that viral replication in this immune compartment serves as a viral reservoir in individuals with controlled disease.[7] Thus, this immunological site is a critical window that allows better evaluation of cellular responses to SIV infection than circulating lymphocyte profiles alone. The impact of chronic cannabinoid administration on gut mucosal immunity and viral changes during SIV infection is not known. However, the presence of cannabinoid receptors (CBR) in the myenteric and submucosal plexus of the gastrointestinal tract[8,9] suggests a potential role for cannabinoids in modulating gastrointestinal responses to infection. Cannabinoids have been demonstrated to modulate gastrointestinal functions including gastrointestinal motility, intestinal secretion, and gastric acid secretion.[10,11] In particular, the type-2 cannabinoid receptor (CB2R) has been linked directly to anti-inflammatory effects in the gastrointestinal tract. This raises the possibility that cannabinoids may modulate gastrointestinal flora and the GALT immunophenotype,[12] a notion that is also supported by studies showing the efficacy of high doses of cannabinoid agonists on inhibition of inflammatory responses associated with colitis.[13–16] We hypothesized that cannabinoid immunomodulatory effects may confer gastrointestinal protection from localized activation of inflammation in SIV-infected animals, potentially reducing tissue injury associated with enhanced viral replication in GALT. The aim of this study was to investigate the consequences of chronic THC administration on gut-localized mechanisms of host response to SIV infection in male rhesus macaques. A systems biology approach was used to identify salient pathways and networks of functional modifications, their correlation with viral kinetics, and their functional significance as they pertain to host–pathogen interactions involved in SIV disease progression.

Materials and Methods

All experiments were approved by the Institutional Animal Care and Use Committee at Louisiana State University Health Sciences Center in New Orleans and adhered to the NIH Guide for the Care and Use of Laboratory Animals. Four- to six-year-old male Rhesus monkeys *(Macaca mulatta)* obtained from the New Iberia Primate Center, LA, were housed individually in aluminum cages (BREC, Inc., Bryan, TX) in a Biosafety Level-2 (BSL-2) containment room maintained on a 12h:12h light–dark cycle at approximately 22°C with 30–70% relative humidity. Animals were fed standard primate chow (Formula 2050, Harlan Teklad, Madison, WI), vitamins, and fruits.

Animal selection criteria

Health status was determined by (1) a complete physical examination performed by a veterinarian, (2) a complete blood count (CBC) and serum chemistries, and (3) negative status for simian retrovirus [Genetic amplification (nested polymerase chain reaction, PCR) of DNA, enzyme immunoassay, and Western immunoblot], and simian T-lymphotropic virus-1 (EIA and Western immunoblot) based on assays performed by the Pathogen Detection Laboratory (California National Primate Research Center, Davis, CA). To reduce and refine the use of nonhuman primates in our research project, *in vitro* assessment of viral kinetics was used to stratify animals according to the rate of peripheral blood mononuclear cell (PBMC) infectivity.[2,17] The rate of *in vivo* disease progression has been correlated to the capacity of PBMCs to express reverse transcriptase activity following *in vitro* infection. Using this information, slow and fast progressors were equally distributed across the vehicle-treated (VEH) ($N=4$) or cannabinoid-treated (THC) ($N=4$) groups, achieving a more homogeneous cohort for study based on viral replication kinetics. This approach has been used previously to decrease variability between the experimental groups and enhance the ability to evaluate the impact of cannabinoid use as a cofactor of disease progression in our sample size.[2,18]

Cannabinoid administration and blood and tissue sampling

After a 3-month quarantine period, training on a behavioral procedure, and the establishment of acute dose–effect curves for THC in all of the subjects, they were divided into two groups, and chronic THC or vehicle (VEH) administration was initiated. THC was obtained from the National Institute on Drug Abuse (Research Technical Branch, Rockville, MD) in 100% ethanol at a concentration of 200 mg/ml. Upon arrival, this solution was lyophilized, stored in aliquots at −20°C, and prepared as an injectable emulsion using alcohol, emulphor, and saline (1:1:18) when needed. Chronic administration of THC occurred twice daily at 8:00 a.m. and 6:00 p.m., and was incremented from 0.18 to 0.32 mg/kg over a 2-week period. The chronic dose remained 0.32 mg/kg thereafter. Intramuscular administration was chosen to reduce experimental variability. This protocol of THC administration produces similar neurobehavioral disruptions as seen following smoked marijuana in humans and produces tolerance to these disruptions over time.[19] Time-matched controls received intramuscular injections of equal volumes (0.05 ml/kg) of vehicle. Care was taken to avoid repeated injections in the same site on an animal's leg to reduce the risk of inflammation or necrosis. This protocol of administration was well tolerated by the animals. These animals were used in previous studies of THC-mediated alterations in lymphocyte subpopulations.[20]

Approximately 17 months (range 14.2–17.0 months; average 16.6 ± 0.83) after initiating chronic THC or VEH administration, blood samples and duodenal biopsies were obtained for determination of lymphocyte populations. Briefly, animals were anesthetized, intubated, and maintained with isoflurane throughout the procedure. Heart rate and oxygen saturation were monitored throughout the procedure. An 8.6-mm flexible endoscope (GIF-Q180, Olympus America, Inc.) was passed through a mouth gag and directed down the esophagus into the stomach. The stomach was distended with air to aid in visualization of the pylorus. The endoscope was directed through the pylorus into the small intestine. Once past the major duodenal papilla, gut mucosal biopsies were obtained with a 2.4-mm biopsy instrument by inserting it through the biopsy channel of the endoscope and into the duodenum.

SIV infection

Animals were inoculated intravenously with a 100 $TCID_{50}$ dose of SIV_{MAC251} (50% tissue culture infective dose). The progression of SIV disease was monitored throughout the study period with clinical and biochemical parameters. Following SIV infection, only one of the VEH/SIV animals

developed clinical signs of disease including weight loss greater than 5% of basal, secondary infections that required antibiotic treatment, neurological manifestations of disease, severe diarrhea, or dehydration at approximately 5 months postinfection. All animals were euthanized at this time point, and a general necropsy was performed as previously described.[19] At necropsy, duodenal samples were excised, washed with phosphate-buffered saline (PBS) supplemented with penicillin and streptomycin, and either used for cell isolation, flash-frozen for later analysis, or fixed in zinc-buffered formalin and embedded for immunohistochemistry and histology. In further attempts to reduce and refine the numbers of nonhuman primates used, duodenal samples were also obtained from three male rhesus macaques that had not been infected with SIV or treated with THC and were euthanized as part of a separate study (Tissues provided by Dr. Peter Didier, Tulane National Primate Research Center). These tissues were used as controls for the microarray analysis.

Duodenal cell isolation

Duodenal samples obtained endoscopically and those collected at the time of necropsy were collected in RPMI-5 (RPMI 1640 supplemented with 100 U/ml penicillin, 100 μg/ml streptomycin, 2 mM glutamine, 25 mM HEPES, and 5% FBS) on ice and used for determination of lymphocyte populations by flow cytometry. The tissue was washed with complete Hanks' balanced salt solution (Hanks' balanced salt solution supplemented with 100 U/ml penicillin, 100 μg/ml streptomycin, 2 mM glutamine, 25 mM HEPES, and 5 mM EDTA) and incubated on a rocker at 37°C in an atmosphere of 5% CO_2 for 30 min. Tissue samples were then centrifuged, resuspended in serum-free complete RPMI with 60 U/ml collagenase, and incubated on a rocker at 37°C in an atmosphere of 5% CO_2 for 60 min. Tissue samples were then centrifuged, resuspended in RPMI-5, and filtered. Duodenal lymphocytes were isolated for flow cytometry using Percoll density gradient centrifugation. All reagents for cell isolations were purchased from Gibco (Invitrogen, Carlsbad, CA).

Flow cytometry

Complete and differential blood counts were performed using a Beckman Coulter LH755 for total leukocyte counts and Wright–Giemsa staining of blood smears for leukocyte differentials. Blood lymphocyte and duodenal subsets were determined by flow cytometric analysis using monoclonal antibodies and isotype controls. Antibodies were purchased from BD Biosciences (San Jose, CA), with the exception of antihuman CD4 (eBioscience, San Diego, CA). Erythrocytes were lysed using Lysis Buffer (BD Biosciences) according to the manufacturer's instructions and samples were washed twice with PBS. Samples were fixed with 1% paraformaldehyde in preparation for analysis. Cells were acquired by the LSUHSC Comprehensive Alcohol Research Center Core Laboratory on a BD LSRII flow cytometer (BD Biosciences), and analysis was performed using FACSDIVA version 6.1.3 software (BD Biosciences) (Figure 1).

Viral quantification

Plasma and tissue viral loads were determined by a quantitative real-time PCR assay (qPCR) that targets a highly conserved region of SIV *gag* in blood samples obtained at discreet time points post-SIV inoculation and in duodenal tissue samples obtained through endoscopy prior to SIV infection and at necropsy. Virus particles were isolated from 1 ml plasma by centrifugation at $20{,}000 \times g$ for 60 min, and viral RNA was purified with Trizol reagent (Life Technologies, Grand Island, NY) according to the manufacturer's directions and resuspended in 30 μl water. For the isolation of RNA from tissues, flash-frozen samples of duodenal tissue were homogenized in Trizol reagent, purified, and resuspended in water at approximately 20 ng/μl. DNA was isolated from tissues and from cryopreserved PBMCs using a Wizard genomic DNA isolation kit (Promega, Madison WI), and approximately 80 ng of total DNA was added to each of the duplicate qPCR assays to determine proviral levels.

For measures of viral RNA, one-tenth of the total RNA isolated from plasma samples and 50–100 ng of RNA prepared from tissue samples were assayed in duplicate reverse-transcriptase qPCR reactions (RT-qPCR). Samples were reverse-transcribed using a TaqMan Gold RT-PCR kit (Applied Biosystems, Life Technologies, Grand Island, NY), which contained Multiscribe reverse transcriptase and random hexamers. The 10 μl reaction was incubated at 25°C for 10 min and 95°C for 5 min to generate cDNA. SIV targets were amplified by overlaying each cDNA with a master mix (15 μl) containing TaqMan Gold reagents (Applied Biosystems), as well as 450 nM SIV *gag* specific forward and reverse primers and 200 nM FAM-labeled SIV *gag* probe onto the RT reaction (Table 1). DNA measures were done similarly, with omission of the RT step, using 25 μl total reaction volume.

Amplification was performed in an ABI 7300 RT-PCR detection system (Applied Biosystems) with an initial incubation at 95°C for 10 min, followed by 40 cycles of 95°C for 15 s and 60°C for 60 s. The threshold cycle (C_t) at which fluorescence was greater than background was identified, and the SIV copy number in each sample was determined by extrapolation from a standard curve generated from serial dilutions of either an SIV *gag* RNA or DNA template. Viral RNA levels in tissue or PBMCs were normalized to measures of rhesus GAPDH mRNA (TaqMan gene expression assay #891279, Applied Biosystems) in the sample, and were expressed as SIV RNA copies/μg mRNA. Proviral levels were normalized to cell numbers using a DNA target present at two copies/cell (RNase P TaqMan control reagents #4316844, Applied Biosystems) and expressed as proviral SIV copies per 10^5 cells. The RNA and DNA qPCR assays have been validated to have a sensitivity of one copy, with the limit of reproducible quantification at five copies of SIV/reaction in the background of either 100 ng of DNA or RNA. This translates to a quantification limit of 50 copies SIV/ml of plasma, 50 copies SIV/μg mRNA, or 50 proviral copies in 10^5 cells. For statistical comparisons, viral loads were $\log_{10}$ transformed.

Microarray

All genomic analyses were done at the LSUHSC/LCRC Genomic Facility. Total RNA was extracted from frozen duodenal tissues using an RNeasy minikit (Qiagen, Valencia, CA) according to the manufacturer's instructions. RNA quantity and quality were assessed by NanoDrop v.3.3.1 (Thermo scientific, Wilmington, DE) and by the Agilent 2100 BioAnalyzer, respectively, prior to hybridizing to Illumina

Table 1. Quantitative Polymerase Chain Reaction Primers and Simian Immunodeficiency Virus Probe

Gene symbol	*Forward (5′ to 3′)*	*Reverse (5′ to 3′)*
SIV		
SIV *gag*	GCGTCATTTGGTGCATTCAC	TCCACCACTAGATGTCTCTGCACTAT
SIV *gag* Probe	6FAM-TGTTTGCTTCCTCAGTATGTTTCACTTTCT CTTCTG-TAMRA	
Rhesus		
RPS13	CTGACGACGTGAAGGAGCAGATT	TCTC TCAGGATCACACCGATTTGT
MX-1	ACCATCGGAATCTTGACGAAGCCT	TGTAGCCCTTCTTCAGGTGGAACA
IFIT-1	AATTCACAGCAACCATGAGTACAAA	GGCTAGTAGGTTGTGTATTCCCAC
MYLK	TTCCATCCAAGGTTTGGACAGTGC	TTACATTGGTCACCTCCCTCCTGA
HSPA2	TGCAGGATTTCTTCAACGGCAAGG	CACATTCTCCGATTTGTCGCCGAT
IGJ	ACATCCGAATTATTGTTCCTCTGA	GGTCTCTGTAGCACTGTCTTCATC

SIV, simian immunodeficiency virus.

HumanWG6_v3 chips, following the manufacturer's instructions and as previously described.[20] After removing the background noise obtained by irrelevant probes ($p < 0.05$), we obtained close to 6,100 genes relevant to the experiment. The signal was normalized using the cubic spline algorithm, which assumes that target signal intensity is normally distributed among replicates of the same condition, and the groups were compared using the Illumina Custom algorithm with multiple testing corrections using the Benjamini–Hochberg false discovery rate (FDR) method. The comparison of the treatment groups (THC/SIV and VEH/SIV) was based on the ratio between their signals and the signal of the tissues from control animals (non-THC, non-SIV). Additional analysis was performed directly comparing gene

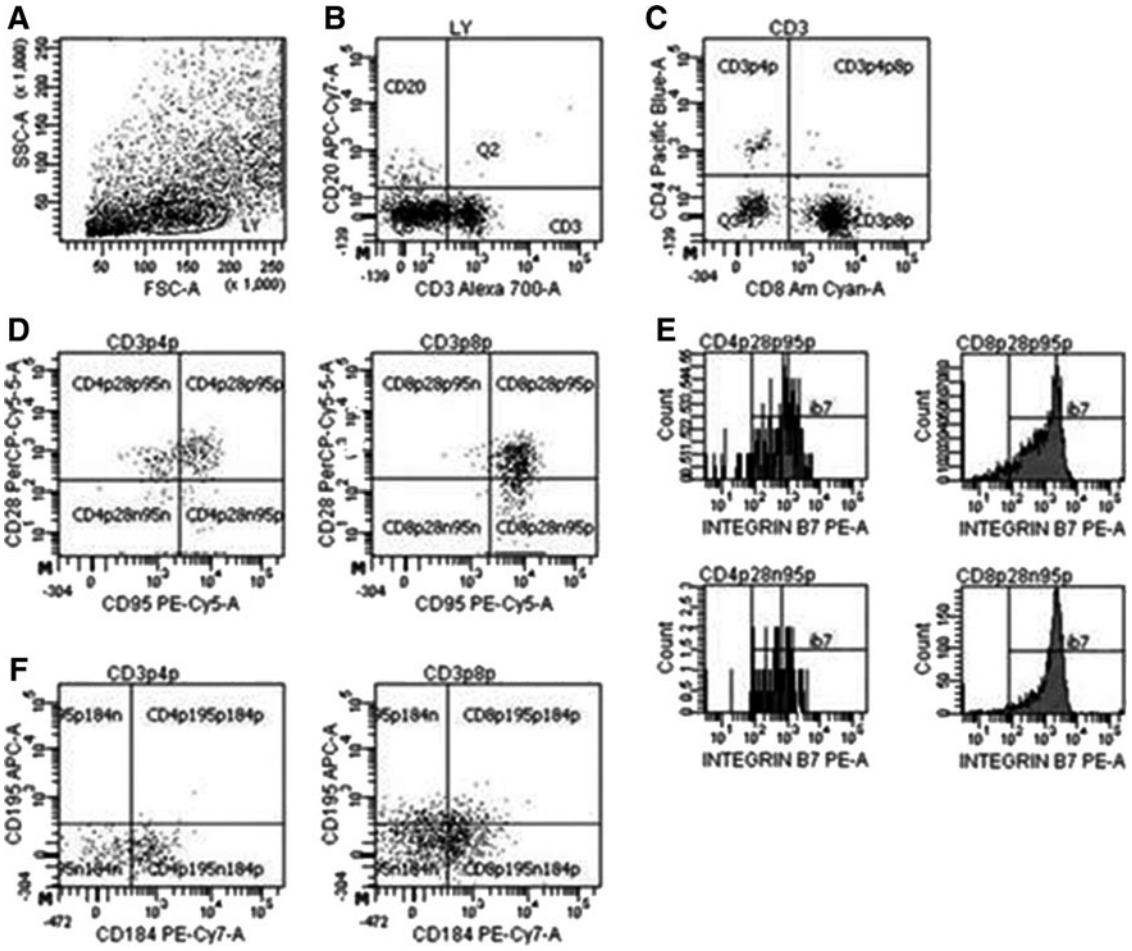

FIG. 1. Representative FACS plots of gating strategy of duodenal T cell populations. Lymphocytes (LY) were first gated on forward and side scatters **(A)**, followed by CD3 versus CD20 **(B)** to eliminate B lymphocytes. $CD3^+$ cells were then distinguished as either $CD4^+$ or $CD8^+$ **(C)** T cells. Central memory ($CD95^+CD28^+$) and effector memory ($CD95^+CD28^-$) $CD4^+$ and $CD8^+$ T lymphocytes **(D)** were further analyzed for integrin $\beta 7$ expression **(E)**. Chemokine receptors CXCR4 (CD184) and CCR5 (CD195) expression was also quantified for both $CD4^+$ and $CD8^+$ T lymphocytes **(F)**.

expression in the THC/SIV vs. VEH/SIV groups. Metacore software (Thomson Reuters, Philadelphia, PA) was used to compare the differentially expressed gene profiles in both groups based on ratios less than 0.5 and higher than 2.0, as described previously.[21] Gene Ontology analysis was conducted to elucidate biological processes enriched with the genes found to be differentially expressed in duodenal tissues from THC/SIV versus VEH/SIV animals.

Duodenal cytokine content determination by Luminex-based multiplex immunoassay

Luminex immunoassays were carried out using a nonhuman primate multiplex cytokine assay kit (Millipore, Billerica, MA) according to the manufacturer's recommended protocols and as previously used by our laboratory.[2]

Immunohistochemistry/confocal microscopy

For immunofluorescence studies, 6-μm formalin-fixed, paraffin-embedded tissue sections were first deparafinized, rehydrated in a descending series of ethanol, and pretreated in a microwave with citrate buffer (antigen unmasking solution; Vector Laboratories, Burlingame, CA) for 20 min at high power according to the manufacturer's instructions. Sections were stained with the appropriate primary and secondary antibody as well as hematoxylin and eosin to microscopically assess the histological status of the tissue. Briefly, slides were blocked with 100 μl of blocking buffer (10 mM Tris–HCl, pH 7.5, 150 mM NaCl, 3% BSA, 10% normal goat serum, and 0.1% Triton X-100) for 1 h followed by a 1-h incubation at room temperature with rabbit polyclonal active caspase-3 primary antibody (1:200 dilution) (Abcam, Cambridge, MA). The slides were washed three times in buffer (10 mM Tris–HCl, pH 7.5, 150 mM NaCl, and 0.1% Triton X-100) followed by the addition of goat antirabbit secondary antibody conjugated to Alexa fluor 488 (1:1,000; Life Technologies, CA). This was followed by mouse anticytokeratin (IgG1 cytokeratin at 1:25; Biocare Medical, Concord, CA) at room temperature for 1 h. The slides were washed three times and incubated for 1 h with goat antimouse secondary antibody conjugated with Alexa Fluorophor 568 (1:1,000). Slides were also incubated with ToPro3 (1 in 1,000) to stain nuclei. Confocal microscopy was performed using a Leica TCS SP2 confocal microscope equipped with three lasers (Leica Microsystems, Exton, PA). Individual optical slices represent 0.2 μM and 32–62 optical slices were collected at 512×512 pixel resolution. NIH Image (version 1.62) and Adobe Photoshop (version 7.0) were used to assign colors to the three channels collected: Alexa 568 (Life Technologies, CA) was red, Alexa 488 (Life Technologies, CA) was green, and the differential interference contrast (DIC) image was in gray scale. The three channels were collected simultaneously. Images were reviewed and scored by a blinded investigator.

Statistical analysis

All data are presented as mean $\pm$ SEM for control ($N=3$), VEH/SIV ($N=3$–4), or THC/SIV ($N=4$). For viral load ($\log_{10}$ transformed values), CBC, cytokine expression, and flow cytometric data, significant differences between VEH/SIV and THC/SIV values at pre-SIV and at necropsy time points were established by two-tailed unpaired Student's *t*-test.

Results

SIV infection

Approximately 17 months after receiving chronic THC or VEH administration, male rhesus macaques were inoculated intravenously with SIV_{MAC251}. The progression of SIV disease was monitored throughout the study period via clinical and biochemical parameters. Circulating viral load in the THC/SIV and VEH/SIV animals averaged 5.2 ± 0.5 and 5.8 ± 0.4 log SIV RNA copies/ml, respectively, at 2 months postinfection (data not shown). At the time of necropsy, plasma viral loads were increased over those measured at set point by 1 log in the VEH/SIV animals, while a more modest average increase of 0.55 log was observed in the THC/SIV group. PBMC proviral load was also lower in THC/SIV animals at necropsy (2.6 ± 0.1 versus 3.0 ± 0.2 log/10^5 cells) (Fig. 2). Similarly, in duodenal tissue samples obtained at

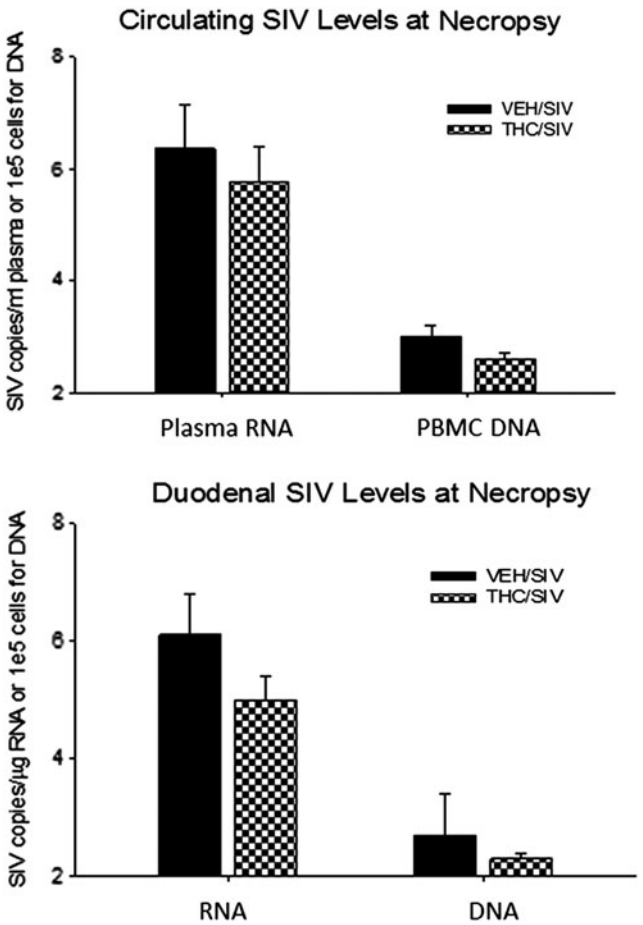

FIG. 2. (Top) Circulating (plasma and peripheral blood mononuclear cells, PBMCs) and (bottom) duodenal tissue viral load (virion RNA and proviral DNA). Viral measures were normalized to micrograms of total mRNA determined with a quantitative polymerase chain reaction (qPCR) assay for GAPDH or cell number (for DNA) using a qPCR assay for a cellular gene. Values are mean $\pm$ SEM [log simian immunodeficiency virus (SIV) RNA copies/μg RNA and log proviral copies/1e5 cells; respectively] in vehicle (VEH)/SIV (filled bars) and Δ^9-tetrahydrocannabinol (THC)/SIV (checkered bars) at necropsy (5 months post-SIV inoculation); $N=4$ in each group.

Table 2. Histopathological Findings at Necropsy

Animal (group)	*Histopathological findings*
A1R035 VEH/SIV	Lymphadenopathy with granulomatous inflammation, pulmonary granulomatous inflammation, steatohepatitis
A1R067 VEH/SIV	Hepatic steatosis, mild pulmonary edema
A1R045 VEH/SIV	CMV enteritis, mild steatohepatitis
A2L046 VEH/SIV	Pulmonary edema and congestion, gastritis, acute bronchopneumonia, CMV meningoencephalitis
A1R071 THC/SIV	Hepatic steatosis, renal infarct
A1R039 THC/SIV	Acute and chronic prostatitis, hepatic steatosis
A1R078 THC/SIV	Mild acute steatohepatitis
A2R116 THC/SIV	Focal mild acute steatohepatitis

VEH, vehicle; SIV, simian immunodeficiency virus; CMV, cytomegalovirus; THC, Δ^a-tetrahydrocannabinol.

necropsy, mean SIV RNA levels were 1 log lower in the THC/SIV group (5.0 ± 0.4 vs. 6.1 ± 0.7 RNA log copies/μg tissue mRNA) with proviral DNA copies also reduced in THC/SIV animals compared to VEH/SIV animals (2.3 ± 0.7 vs. 2.7 ± 0.7 log viral copies/10^5 cells). Differences in viral load and proviral DNA levels did not reach statistical significance.

Only one of the animals (VEH/SIV) met the clinical criteria for necropsy. Histopathological examination revealed more frequent evidence of an immunocompromised status in the VEH/SIV (3/4) animals than in the THC/SIV groups (0/4) (Table 2). Specifically, one VEH/SIV animal showed CMV inclusions in duodenal tissue (Fig. 3).

Complete and differential blood counts and lymphocyte subsets

Overall, chronic THC treatment did not result in significant modulation of peripheral white blood cell count, differential, or hematocrit values (Table 3). Administration of THC for 17 months resulted in more peripheral blood $CXCR4^+CD8^+$ ($p = 0.057$) cells as compared to vehicle controls, and less duodenal tissue $CCR5^+CD8^+$ cells (Tables 4 and 5). Otherwise, no significant differences in lymphocyte subpopulations were noted prior to SIV infection.

SIV infection resulted in a marked 30% drop in percent circulating $CD4^+$ T cells in both THC/SIV and VEH/SIV animals by 2 months (data not shown). In duodenum, the $\%CD4^+$ T cells was approximately 85% lower than pre-SIV values in gut pinch biopsies obtained from both experimental groups (data not shown). At necropsy ($\sim$5 months post-SIV), there were no differences between VEH/SIV and THC/SIV groups in the number of peripheral blood $CD4^+$ or $CD8^+$ T lymphocytes, the CD4/CD8 ratio, or in CCR5 or CXCR4 surface expression on these cells (Table 4). Duodenal lymphocyte populations isolated from intact tissue at the time of necropsy showed significantly higher duodenal $CD4^+$ central memory T cells (T_{CM}; $CD95^+CD28^+$) $\beta7^+$, and $CD8^+$ T_{CM} in the THC/SIV versus the VEH/SIV animals. Otherwise, there were no significant differences in duodenal tissue $CD4^+$ or $CD8^+$ T lymphocyte counts or subsets between VEH- and THC-treated animals prior to SIV infection or at the time of necropsy.

Duodenal cytokine expression

At the time of necropsy, duodenal tissue showed significantly higher expression of interleukin (IL)-4, IL-5, IL-6, and IL-13 in the THC/SIV animals than those of VEH/SIV animals (Table 6). A similar trend was observed for IL-2, tumor necrosis factor (TNF)-α, and vascular endothelial growth factor (VEGF), but the differences failed to reach statistical significance.

Gene microarray

Using an Illumina Custom algorithm to compare gene expression (p-value filter of ≤ 0.05), up-regulated ($N = 96$; >2-fold higher) or down-regulated ($N = 178$; >2-fold lower) genes were identified in gut samples from the VEH/SIV and control

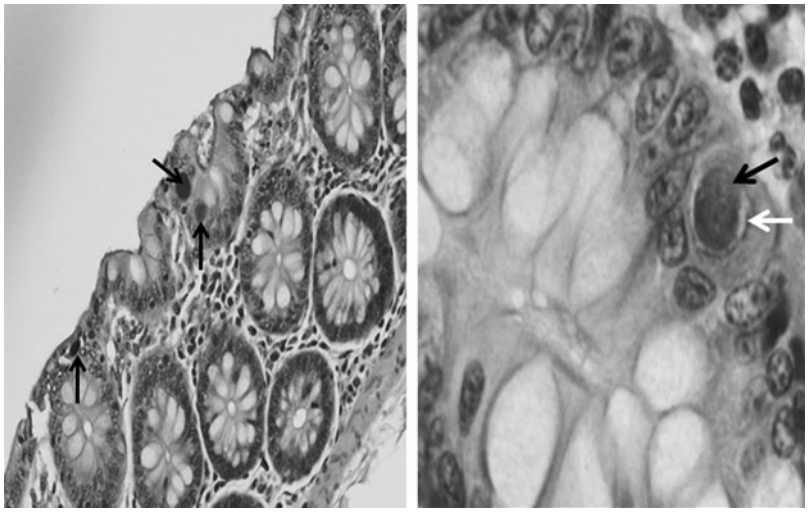

FIG. 3. Histologic section of VEH/SIV animal duodenum sampled at necropsy showing large, basophilic, intranuclear viral inclusions (black arrows) associated with adjacent perinuclear clear zones (white arrow) characteristic of cytomegalovirus (CMV) enteritis [left at 10×; right at 40×; hematoxylin and eosin (H&E) stain].

TABLE 3. WHITE BLOOD CELL COMPLETE AND DIFFERENTIAL COUNTS

Complete blood count	*VEH/SIV*	*THC/SIV*	p
White blood cells ($\times 10^3/\mu$l)	4.4 ± 0.8	5.3 ± 1.5	0.627
Neutrophils ($\times 10^3/\mu$l)	2.2 ± 0.2	3.3 ± 1.2	0.476
Lymphocytes ($\times 10^3/\mu$l)	1.7 ± 0.6	1.3 ± 0.2	0.461
Monocytes ($\times 10^3/\mu$l)	0.3 ± 0.0	0.3 ± 0.0	0.635
Eosinophils ($\times 10^3/\mu$l)	0.2 ± 0.1	0.4 ± 0.2	0.354
Hemoglobin (g/dl)	12.1 ± 0.9	12.5 ± 0.3	0.622
Hematocrit (%)	39.2 ± 3.4	39.6 ± 0.9	0.901
Platelets ($\times 10^3/\mu$l)	307.3 ± 42.3	198.3 ± 52.3	0.186

White blood cell complete and differential counts in vehicle- and THC-treated SIV-infected rhesus macaques at necropsy. Values are presented as mean ± SEM for VEH/SIV ($N = 3$) and THC/SIV ($N = 4$) animals.

TABLE 4. LYMPHOCYTE POPULATIONS

	VEH/SIV	*THC/SIV*	p
Pre-SIV inoculation			
Lymphocyte type (%CD3)			
$CD3^+$ $CD4^+$	54.1 ± 2.2	59.8 ± 4.7	0.333
$CD3^+$ $CD8^+$	36.9 ± 1.4	33.5 ± 3.7	0.437
CD4/CD8	1.5 ± 0.1	1.9 ± 0.5	0.335
$CD4^+$ memory subtypes (%CD4)			
$CD95^+$ $CD28^+$	48.1 ± 10.2	45.3 ± 5.8	0.824
$CD95^+$ $CD28^-$	7.2 ± 1.4	6.2 ± 1.1	0.601
$CD8^+$ memory subtypes (%CD8)			
$CD95^+$ $CD28^+$	24.8 ± 5.7	25.2 ± 4.7	0.956
$CD95^+$ $CD28^-$	28.9 ± 3.8	25.5 ± 3.8	0.554
$CD4^+$ chemokine receptors (%CD4)			
Total $CCR5^+$	8.2 ± 3.8	6.5 ± 2.2	0.735
Total $CXCR4^+$	46.3 ± 7.1	55.4 ± 3.6	0.332
$CD8^+$ chemokine receptors (%CD8)			
Total $CCR5^+$	22.4 ± 5.4	18.1 ± 5.7	0.611
Total $CXCR4^+$	24.3 ± 4.6	40.3 ± 4.3	0.057
At necropsy			
Lymphocyte type (%CD3)			
$CD3^+$ $CD4^+$	39.8 ± 10.6	34.4 ± 6.2	0.688
$CD3^+$ $CD8^+$	49.9 ± 13.0	59.6 ± 6.9	0.555
CD4/CD8	1.1 ± 0.6	0.6 ± 0.1	0.525
$CD4^+$ memory subtypes (%CD4)			
$CD95^+$ $CD28^+$	29.0 ± 4.2	28.7 ± 2.0	0.969
$CD95^+$ $CD28^-$	29.6 ± 15.1	14.5 ± 2.0	0.421
$CD8^+$ memory subtypes (%CD8)			
$CD95^+$ $CD28^+$	25.4 ± 1.5	30.4 ± 3.1	0.219
$CD95^+$ $CD28^-$	48.0 ± 11.3	43.6 ± 3.0	0.737
$CD4^+$ chemokine receptors (%CD4)			
Total $CCR5^+$	1.9 ± 0.8	2.6 ± 0.4	0.501
Total $CXCR4^+$	73.6 ± 9.3	72.0 ± 8.6	0.903
$CD8^+$ chemokine receptors (%CD8)			
Total $CCR5^+$	14.7 ± 3.1	18.6 ± 8.0	0.674
Total $CXCR4^+$	49.5 ± 12.8	39.5 ± 1.9	0.519

Peripheral blood lymphocyte subsets, memory status, proliferation, and chemokine receptor expression indices in cells isolated from vehicle- and THC-treated SIV-infected rhesus macaques from pre-SIV and necropsy. Values (percent of the parent population) are presented as mean ± SEM for VEH/SIV ($N = 3$) and THC/SIV ($N = 4$) animals.

TABLE 5. DUODENAL LYMPHOCYTE POPULATIONS

	VEH/SIV	*THC/SIV*	p
Pre-SIV inoculation			
Lymphocyte type (%CD3)			
$CD3^+CD4^+$	9.1 ± 3.3	11.6 ± 0.6	0.531
$CD3^+CD8^+$	66.9 ± 1.8	63.7 ± 5.0	0.588
CD4/CD8	0.1 ± 0.05	0.2 ± 0.02	0.439
$CD4^+$ memory subtypes (%CD4)			
$CD95^+CD28^+$	50.0 ± 5.0	55.0 ± 5.3	0.524
$CD95^+CD28^+$ $\beta7^+$	47.9 ± 5.5	48.5 ± 3.2	0.932
$CD95^+CD28^-$	41.9 ± 4.6	38.3 ± 6.4	0.671
$CD95^+CD28^-$ $\beta7^+$	39.7 ± 3.8	35.9 ± 8.0	0.932
$CD8^+$ memory subtypes (%CD8)			
$CD95^+CD28^+$	26.0 ± 2.1	31.8 ± 0.5	0.104
$CD95^+CD28^+$ $\beta7^+$	25.8 ± 2.1	31.5 ± 0.4	0.105
$CD95^+CD28^-$	61.2 ± 3.7	61.9 ± 1.0	0.867
$CD95^+CD28^-$ $\beta7^+$	60.9 ± 3.7	61.7 ± 1.1	0.852
$CD4^+$ chemokine receptors (%CD4)			
Total $CCR5^+$	44.0 ± 1.0	34.5 ± 9.3	0.382
Total $CXCR4^+$	15.3 ± 1.3	24.4 ± 6.4	0.250
$CD8^+$ chemokine receptors (%CD8)			
Total $CCR5^+$	32.4 ± 0.5	19.0 ± 2.3	0.008
Total $CXCR4^+$	24.3 ± 4.6	23.1 ± 2.4	0.830
At necropsy			
Lymphocyte type (%CD3)			
$CD3^+CD4^+$	12.94 ± 12.5	10.1 ± 8.2	0.861
$CD3^+CD8^+$	66.21 ± 23.9	79.6 ± 12	0.652
CD4/CD8	0.68 ± 0.7	0.2 ± 0.3	0.562
$CD4^+$ memory subtypes (%CD4)			
$CD95^+CD28^+$	25.47 ± 17.8	46.9 ± 9.4	0.363
$CD95^+CD28^+$ $\beta7^+$	2.85 ± 2.9	21.7 ± 4.4	0.017
$CD95^+CD28^-$	66.31 ± 18.1	21.9 ± 3.7	0.129
$CD95^+CD28^-$ $\beta7^+$	41.33 ± 29.5	11.9 ± 6.5	0.424
$CD8^+$ memory subtypes (%CD8)			
$CD95^+CD28^+$	18.76 ± 2.1	28.0 ± 2.8	0.045
$CD95^+CD28^+$ $\beta7^+$	11.70 ± 2.1	18.4 ± 3.9	0.200
$CD95^+CD28^-$	48.19 ± 2.9	49.2 ± 4.0	0.868
$CD95^+CD28^-$ $\beta7^+$	36.07 ± 6.1	36.7 ± 6.8	0.948
$CD4^+$ chemokine receptors (%CD4)			
Total $CCR5^+$	6.73 ± 4.3	12.4 ± 5.0	0.431
Total $CXCR4^+$	10.61 ± 6.0	24.9 ± 10.5	0.295
CD8 + chemokine receptors (%CD8)			
Total $CCR5^+$	32.02 ± 12.0	36.9 ± 4.8	0.737
Total $CXCR4^+$	33.37 ± 16.4	21.7 ± 6.3	0.561

Duodenal lymphocyte subsets, memory status, proliferation, and chemokine receptor expression within lymphocyte populations isolated from vehicle- and THC-treated SIV-infected rhesus macaques at pre-SIV and necropsy. Values (percent of the parent population) are presented as mean ± SEM.

groups. Of these, six genes (*PPP1R1A*, *PRSS23*, *ZNF358*, *PRSS7*, *KIAA0427*, *PLEKHO1*) were significantly ($p < 0.05$) different between the tissues of the THC/SIV and VEH/SIV groups. Using gene ontology analysis, 10 cellular physiological processes or signal transduction pathways were identified as significantly enriched by these genes (Table 7). These findings were indicative of specific major domains that could be differentially modulated by THC in the SIV-infected animals: (1) regulation of apoptosis, (2) cell survival, proliferation and morphogenesis, and (3) energy and substrate metabolic regulation.

Additional analysis contrasting gene expression in VEH/SIV vs. THC/SIV showed 93 genes differentially expressed between THC/SIV and VEH/SIV animals. Of these, 45 were

Table 6. Cytokine Content of Duodenal Tissue at Necropsy

Cytokine	*VEH/SIV (pg/mg)*	*THC/SIV (pg/mg)*	p
G-CSF	17.5 ± 2.8	47.8 ± 17.6	0.164
GM-CSF	3.7 ± 1.0	11.7 ± 6.4	0.288
IFNγ	8.0 ± 2.7	15.8 ± 3.2	0.133
IL-1B	2.9 ± 1.5	3.8 ± 0.6	0.613
IL-1ra	142.6 ± 59.5	120.2 ± 13.1	0.732
IL-2	2.6 ± 0.2	5.0 ± 0.9	0.056
IL-4	10.4 ± 3.7	27.8 ± 1.8	0.014
IL-5	2.0 ± 1.2	9.6 ± 1.9	0.028
IL-6	1.2 ± 0.2	2.8 ± 0.2	0.009
IL-8	16.3 ± 2.7	18.9 ± 4.7	0.652
IL-10	164.1 ± 98.0	343.5 ± 81.7	0.232
IL-12/23	16.2 ± 7.3	23.5 ± 4.6	0.444
IL-13	1.7 ± 0.3	4.4 ± 0.8	0.038
IL-15	94.3 ± 37.5	74.9 ± 8.4	0.640
IL-17	2.1 ± 0.8	4.2 ± 0.9	0.159
MCP-1	86.3 ± 9.3	126.2 ± 59.5	0.544
MIP-1β	3.3 ± 0.6	6.0 ± 2.0	0.255
MIP-1α	14.2 ± 1.9	18.1 ± 2.5	0.281
sCD40L	54.6 ± 17.1	78.7 ± 17.0	0.374
TGFα	10.1 ± 3.0	15.6 ± 4.2	0.341
TNFα	66.4 ± 17.1	135.9 ± 21.3	0.064
VEGF	41.5 ± 4.1	73.3 ± 12.7	0.075
IL-18	153.3 ± 123.8	37.9 ± 20.9	0.410

Cytokine concentrations (pg/mg protein) in duodenal tissue obtained from VEH/SIV and THC/SIV groups at necropsy. Values are mean ± SEM. $N = 4–5$/group.

G-CSF, granulocyte colony-stimulating factor; GM-CSF, granulocyte-macrophage colony-stimulating factor; IFN, interferon; IL, interleukin; MCP-1, monocyte chemotactic protein-1; MIP, macrophage inflammatory protein; TGF, tumor growth factor; TNF, tumor necrosis factor; VEGF, vascular endothelial growth factor.

Table 7. Gene Ontology Processes

Rank	*THC/SIV vs. VEH/SIV vs. control*	p *value*
1	Negative regulation of protein kinase B signaling cascade	0.01
2	Intrinsic apoptotic signaling pathway in response to DNA damage by p53 class mediator	0.01
3	Embryonic forelimb morphogenesis	0.01
4	Forelimb morphogenesis	0.02
5	Intrinsic apoptotic signaling pathway in response to DNA damage	0.02
6	Glycogen metabolic process	0.02
7	Cellular glucan metabolic process	0.02
8	Regulation of translational initiation	0.03
9	Glucan metabolic process	0.03
10	Cellular polysaccharide metabolic process	0.04
Rank	*THC/SIV vs. VEH/SIV*	p *value*
1	Regulation of muscle contraction	2.207E-12
2	Muscle contraction	4.975E-10
3	Muscle filament sliding	8.149E-09
4	L-Glutamate uptake involved in synaptic transmission	1.222E-08
5	Cardiac muscle contraction	5.512E-08
6	Muscle organ development	5.900E-08
7	Regulation of cardiac muscle cell contraction	6.247E-08
8	Actin crosslink formation	3.934E-07
9	Positive regulation of oxidative phosphorylation uncoupler activity	6.200E-07
10	Regulation of hormone levels	6.200E-07

Gene ontology processes significantly enriched with genes ($N = 6$) differentially regulated between THC/SIV and VEH/SIV using a control uninfected group as reference (Top). The bottom panel reflects top ranking processes enriched with genes ($N = 93$) differentially regulated in duodenal tissues from THC/SIV vs. those obtained from VEH/SIV animals.

more than 2-fold higher in the THC/SIV animals than in the VEH/SIV animals. Pathway analysis of the 93 differentially expressed genes primarily reflects metabolic processes involved in muscle contraction being the most enriched in the THC/SIV animals (Table 7). Gene network processes included protein folding, cytoskeleton remodeling, cell adhesion, and cell signaling (not shown).

Histology and immunohistochemistry

To obtain functional evidence that THC-mediated modulation of gene expression in duodenal samples exerted antiapoptotic effects, we performed immunofluorescence studies to detect cells that stained positive for active caspase-3. As shown in Fig. 4 for a representative animal from the VEH/SIV group, an increased number of crypt cells stained positive for active caspase-3. In contrast, fewer crypt cells stained positive for active caspase-3 in the duodenum of the representative THC/SIV animal. These results suggest that THC may protect intestinal crypt epithelial cells from apoptosis. Staining for ZO-1 and occludin to determine if THC modulated the intestinal epithelial barrier did not reveal any significant differences between the two groups.

Discussion

This study investigated the modulatory effects of chronic THC administration on gut-localized mechanisms of host response to SIV infection in male rhesus macaques. Our results show that chronic THC administration attenuated the percentages of circulating $CXCR4^+CD8^+$ T lymphocytes and decreased the percentages of duodenal $CCR5^+CD8^+$ T lymphocytes preinfection. Moreover, duodenal tissues from chronic THC-treated SIV-infected macaques had increased duodenal $CD4^+$ T_{CM} ß7^+ and $CD8^+$ T_{CM} lymphocytes, attenuated gut viral load, and a significant shift in cytokine expression favoring a type-2 helper T cell (Th2)-type profile at the time of necropsy. These immunomodulatory effects of chronic THC administration were associated with significant differences in duodenal tissue gene expression, which by gene ontology analysis strongly suggests an overall antiapoptotic and, possibly, proliferative or regenerative effect on the gut tissues. This was partly confirmed with the observation that apoptosis in epithelial crypt cells from THC/SIV animals was markedly less than that seen in VEH/SIV animals. These findings suggest that local gut mechanisms may contribute to chronic THC modulation of SIV disease progression.

Chronic THC administration prior to SIV infection decreased the percentages of the $CCR5^+CD8^+$ duodenal cell population as measured by flow cytometry. CCR5 is a chemokine receptor for β chemokines, RANTES, and macrophage inflammatory protein (MIP)-1α and MIP-1β as well as coreceptor for HIV.[22–24] While the role of CCR5 on $CD4^+$

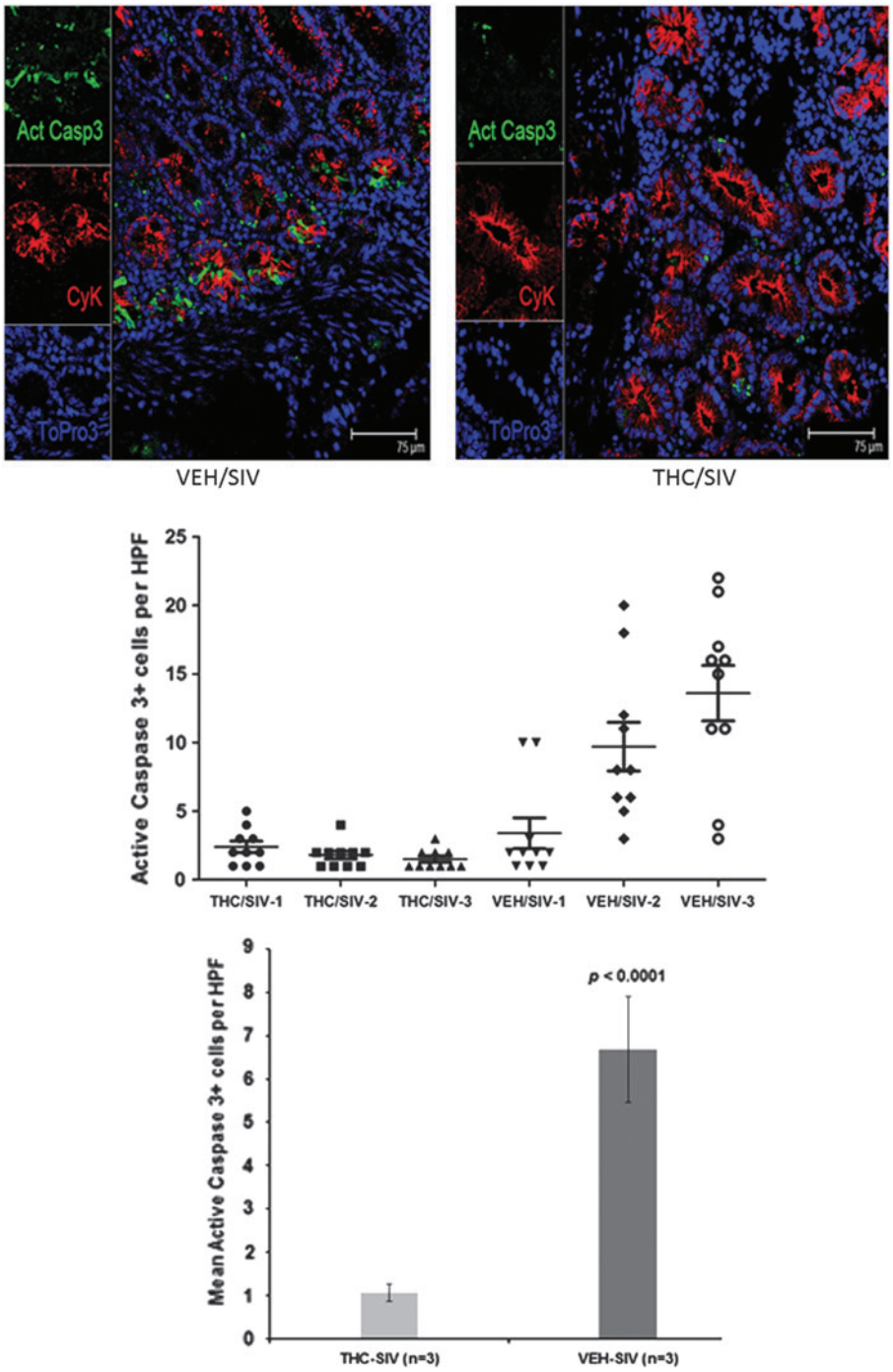

FIG. 4. Immunohistochemical staining for apoptosis in representative duodenal samples from the VEH/SIV and THC/SIV animals. THC decreased the number of apoptotic cells in the duodenal crypts of SIV-infected macaques (bottom) compared to those of VEH/SIV animals (top). Markers shown include active caspase-3 in green, cytokeratin (a marker for epithelial cells) in red, and DAPI staining for nuclei in blue. For each panel the individual channels appear on the left with a merged image on the right.

T cells in HIV infection has been extensively researched, very little is known about the role of $CCR5^+CD8^+$ T cells. CCR5 may facilitate the migration of $CD8^+$ memory cells to sites of inflammation or to lymphoid tissues.[25] The lower percentage of this cell population in the THC/SIV animals could reflect reduced levels of inflammation in subjects chronically treated with THC. In addition, a trend toward greater percentages of $CXCR4^+CD4^+$ T cells was noted in the duodenal tissues of the THC/SIV group at the time of necropsy. These cells are not targets of SIV infection in rhesus macaques.[26] However, $CXCR4^+CD4^+$ T cells may be an important source of $CD4^+$ T cell help and renewal that could potentially improve resistance to SIV infection.

Our results demonstrated that chronic THC administration preserved T_{CM} cell populations and resulted in significantly greater percentages of gut $CD4^+$ and $CD8^+$ T_{CM} cells in the THC/SIV group than the VEH/SIV group at the time of necropsy. This is consistent with the reduced levels of SIV seen in these tissues and the attenuation of SIV disease and improved immunocompetence in the THC-treated group. Maintenance of the central memory T cell pool is critical for continued production of effector memory T cells. SIV exploits the large population of memory $CD4^+$ T cells in the effector arm of GALT as the primary target for replication and depletes this cell population by direct and indirect mechanisms.[27] We speculate that chronic THC administration may directly or

indirectly promote the maintenance of the central memory T cell pool in the gut mucosa, possibly by preservation of T cell homeostasis in these tissues.

Based on our previous observations of attenuated inflammatory cytokine expression in brain tissues of THC/SIV animals,[19] we predicted a similar pattern would emerge in duodenal tissues. In contrast, significantly higher expression of IL-4, IL-5, IL-6, and IL-13 was detected in duodenal tissues of the THC/SIV animals than in those from VEH/SIV animals. A similar trend was observed for IL-2, TNF-α, and VEGF. Overall, this pattern of cytokine expression reflects a shift toward a Th2-type phenotype, consistent with previous reports of cannabinoid-mediated enhancement of Th2 cytokine expression.[28–36] While IL-6 is widely regarded as a proinflammatory cytokine, it also has regenerative and anti-inflammatory properties, and plays a crucial role in the development of particular $CD4^+$ T cell subsets including T follicular helper (TFH) cells, IL-17-secreting $CD4^+$ T cells (Th17 cells), and regulatory T cells (Tregs).[37,38] The preferential expression of Th2 cytokines could have contributed to control of local viral replication, particularly the increase in IL-13 and IL-4, which have been shown to inhibit monocyte production of proinflammatory cytokines and to inhibit HIV-1 replication in macrophages.[39] Thus, the observed cytokine profile, in conjunction with the attenuated viral load in duodenal tissues of THC/SIV animals, suggests an immunomodulatory process that more effectively controlled viral replication. Support for an immunomodulatory role for cannabinoids comes from reports in the literature of protective effects of cannabinoids in other animal models of gastrointestinal inflammation.[13,14,16,40]

In addition to the cytokines discussed above, THC/SIV animals demonstrated nearly 2-fold higher concentrations of IL-17. IL-17 may be produced by a variety of cell populations, including $CD4^+$ Th17 cells, $CD8^+$ Tc17 cells, and innate lymphoid cells. Evidence suggests that subsets of IL-17-secreting cells are important for elite control of HIV and SIV infection.[37,41–44] For example, experimental evidence has suggested a role for IL-17 in the maintenance of gut mucosal integrity and demonstrated that significant depletions of IL-17-secreting cell populations in chronic SIV infection correspond to increased viral load and disease progression.[37,41–44] Healthy nonhuman primates maintain higher frequencies of Th17 cells in the gut mucosa following SIV infection, and once depleted in SIV-infected macaques, these T cell subsets are not reconstituted.[41] Even though the difference in IL-17 content between the THC/SIV and VEH/SIV groups did not reach statistical significance, cannabinoid-mediated effects on IL-17-secreting cell subsets may be a potential mechanism for THC-mediated attenuation of SIV disease progression and warrant further investigation.

Exploratory microarray analysis revealed a significant number of genes to be differentially expressed in the duodenal tissues of SIV-infected animals when compared to tissues of naive uninfected controls. To identify the most salient changes, we limited gene analysis to those that were not only statistically different, but to those for which the difference in expression was 2-fold higher or lower in tissues from SIV-infected animals as compared to tissues from naive control animals. Using that algorithm, only six genes were shown to have differential duodenal expression between the VEH/SIV and THC/SIV groups. Gene ontology analysis identified their significant representation in processes involved in apoptosis and in proliferative or regenerative signaling categories. While we did not confirm gene expression, we obtained functional verification of the relevance of the apoptosis pathway. Expanded analysis of differential gene expression produced a larger number of genes of interest. However, as shown in Table 7, the processes enriched with these genes were less relevant to disease progression than those identified with a more stringent approach.

In line with the processes identified by GeneGo analysis, our results showed increased numbers of active caspase-3-positive cells localizing to the crypt compartment of the duodenum, particularly in VEH/SIV animals. In contrast, very few active caspase-3-positive cells were detected in the duodenal crypts of the THC/SIV animals, suggesting marked protection from apoptosis by THC. These results are in agreement with a recent report describing decreased TNF-α production and a reduction in the amount of cleaved caspase-3 in colonic epithelial cells following cannabidiol treatment in a mouse model of LPS-induced intestinal inflammation.[45] Moreover, these results suggest additional protective roles for cannabinoids on intestinal epithelial cell proliferation and regeneration, maintenance of the integrity of the epithelial layer, and possibly a preservation of intestinal barrier function; however, this remains to be determined.

Disruption of the intestinal barrier has been proposed as a mechanism that facilitates translocation of intestinal bacteria and bacterial products leading to systemic immune activation/inflammation thereby driving AIDS progression.[46] Others have found a role for the endogenous cannabinoid system in the maintenance of intestinal epithelial barrier function,[47] but the work is limited and needs further investigation. Contrary to our expectation, immunofluorescence analysis did not reveal any significant alterations in the expression of ZO-1 or occludin, the principal tight junction proteins responsible for preserving the integrity of the intestinal epithelial barrier. While these results do not directly support a role for cannabinoid modulation of intestinal barrier integrity, the implication of cannabinoids as modulators of barrier function, particularly as it pertains to the blood–brain barrier, warrants further investigation.[48]

In summary, using a systems biology approach to understanding the impact of chronic cannabinoid treatment on gut-associated immunopathology, we identified relevant mechanisms that can potentially modulate disease progression. Our results suggest that gut immunomodulation through changes in gene expression, cytokine profiles, and immune cell populations could potentially contribute to chronic THC modulation of SIV disease progression. Moreover, they reveal novel mechanisms that may potentially contribute to decreased morbidity and mortality.

Acknowledgments

The authors would like to thank Jaime Hubbell, Blake Lewis, Nedra Lacour, Xavier Alvarez, and Constance Porretta for their outstanding analytical support and Whitney Nichols and Drs. Joe Moerschbaecher and Robert Siggins for critical scientific discussions. Tissue samples from naive uninfected male rhesus macaques were kindly provided by Dr. Peter Didier, Tulane National Primate Research Center. Supported by NIH/NIDA R01 DA030053-04, P20GM103501, and NIDA-020419-01A1.

Author Disclosure Statement

No competing financial interests exist.

References

1. U.S. Department of Health and Human Services Substance Abuse and Mental Health Services Administration Center for Behavioral Health Statistics and Quality: Results from the 2011 National Survey on Drug Use and Health: Summary of National Findings. www.samhsa.gov/data/NSDUH/2k11Results/NSDUHresults2011.pdf 2012.
2. Molina PE, Winsauer P, Zhang P, *et al.:* Cannabinoid administration attenuates the progression of simian immunodeficiency virus. AIDS Res Hum Retroviruses 2011;27:585–592.
3. Molina PE, Amedee A, LeCapitaine NJ, *et al.:* Cannabinoid neuroimmune modulation of SIV disease. J Neuroimmune Pharmacol 2011;6:516–527.
4. Dandekar S: Pathogenesis of HIV in the gastrointestinal tract. Curr HIV/AIDS Rep 2007;4:10–15.
5. George MD, Reay E, Sankaran S, and Dandekar S: Early antiretroviral therapy for simian immunodeficiency virus infection leads to mucosal CD4+ T-cell restoration and enhanced gene expression regulating mucosal repair and regeneration. J Virol 2005;79:2709–2719.
6. Ling B, Veazey RS, Hart M, *et al.:* Early restoration of mucosal CD4 memory CCR5 T cells in the gut of SIV-infected rhesus predicts long term non-progression. AIDS 2007;21:2377–2385.
7. Chun TW, Nickle DC, Justement JS, *et al.:* Persistence of HIV in gut-associated lymphoid tissue despite long-term antiretroviral therapy. J Infect Dis 2008;197:714–720.
8. Wright K, Rooney N, Feeney M, *et al.:* Differential expression of cannabinoid receptors in the human colon: Cannabinoids promote epithelial wound healing. Gastroenterology 2005;129:437–453.
9. Kulkarni-Narla A and Brown DR: Localization of CB1-cannabinoid receptor immunoreactivity in the porcine enteric nervous system. Cell Tissue Res 2000;302:73–80.
10. Pertwee RG: Cannabinoids and the gastrointestinal tract. Gut 2001;48:859–867.
11. Izzo AA, Mascolo N, and Capasso F: The gastrointestinal pharmacology of cannabinoids. Curr Opin Pharmacol 2001;1:597–603.
12. Wright KL, Duncan M, and Sharkey KA: Cannabinoid CB2 receptors in the gastrointestinal tract: A regulatory system in states of inflammation. Br J Pharmacol 2008;153:263–270.
13. Kimball ES, Schneider CR, Wallace NH, and Hornby PJ: Agonists of cannabinoid receptor 1 and 2 inhibit experimental colitis induced by oil of mustard and by dextran sulfate sodium. Am J Physiol Gastrointest Liver Physiol 2006;291:G364–G371.
14. Massa F, Marsicano G, Hermann H, *et al.:* The endogenous cannabinoid system protects against colonic inflammation. J Clin Invest 2004;113:1202–1209.
15. Storr MA, Keenan CM, Emmerdinger D, *et al.:* Targeting endocannabinoid degradation protects against experimental colitis in mice: Involvement of CB1 and CB2 receptors. J Mol Med (Berl) 2008;86:925–936.
16. Storr MA, Keenan CM, Zhang H, Patel KD, Makrivannis A, and Sharkey KA: Activation of the cannabinoid 2 receptor (CB2) protects against experimental colitis. Inflamm Bowel Dis 2009;15:1678–1685.
17. Seman AL, Pewen WF, Fresh LF, Martin LN, and Murphey-Corb M: The replicative capacity of rhesus macaque peripheral blood mononuclear cells for simian immunodeficiency virus in vitro is predictive of the rate of progression to AIDS in vivo. J Gen Virol 2000;81:2441–2449.
18. Bagby GJ, Stoltz DA, Zhang P, *et al.:* The effect of chronic binge ethanol consumption on the primary stage of SIV infection in rhesus macaques. Alcohol Clin Exp Res 2003;27:495–502.
19. Winsauer PJ, Molina PE, Amedee AM, *et al.:* Tolerance to chronic delta-9-tetrahydrocannabinol (Δ[9]-THC) in rhesus macaques infected with simian immunodeficiency virus. Exp Clin Psychopharmacol 2011;19(2):154–172.
20. LeCapitaine NJ, Zhang P, Winsauer P, Walker E, Vande Stouwe C, Porretta C, and Molina PE: Chronic Δ-9-tetrahydrocannabinol administration increases lymphocyte CXCR4 expression in rhesus macaques. J Neuroimmune Pharmacol 2011;6(4):540–545.
21. Kim SH, Sierra RA, McGee DJ, and Zabaleta J: Transcriptional profiling of gastric epithelial cells infected with wild type or arginase-deficient Helicobacter pylori. BMC Microbiol 2012;12:175.
22. Venkatesan S, Petrovic A, Locati M, Kim YO, Weissman D, and Murphy PM: A membrane-proximal basic domain and cysteine cluster in the C-terminal tail of CCR5 constitute a bipartite motif critical for cell surface expression. J Biol Chem 2001;276:40133–40145.
23. Berger EA, Murphy PM, and Farber JM: Chemokine receptors as HIV-1 coreceptors: Roles in viral entry, tropism, and disease. Annu Rev Immunol 1999;17:657–700.
24. Littman DR: Chemokine receptors: Keys to AIDS pathogenesis? Cell 1998;93(5):677–680.
25. Fukada K, Sobao Y, Tomiyama H, Oka S, and Takiguchi M: Functional expression of the chemokine receptor CCR5 on virus epitope-specific memory and effector CD8+ T cells. J Immunol 2002;168(5):2225–2232.
26. Edinger AL, Amedee A, Miller K, *et al.:* Differential utilization of CCR5 by macrophage and T cell tropic simian immunodeficiency virus strains. Proc Natl Acad Sci USA 1997;94:4005–4010.
27. Li Q, Duan L, Estes JD, *et al.:* Peak SIV replication in resting memory CD4+ T cells depletes gut lamina propria CD4+ T cells. Nature 2005;434(7037):1148–1152.
28. Newton CA, Klein TW, and Friedman H: Secondary immunity to Legionella pneumophila and Th1 activity are suppressed by delta-9-tetrahydrocannabinol injection. Infect Immun 1994;62:4015–4020.
29. Klein TW, Newton CA, Nakachi N, and Friedman H: Delta 9-tetrahydrocannabinol treatment suppresses immunity and early IFN-gamma, IL-12, and IL-12 receptor beta 2 responses to Legionella pneumophila infection. J Immunol 2000;164:6461–6466.
30. Zhu LX, Sharma S, Stolina M, *et al.:* Delta-9-tetrahydrocannabinol inhibits antitumor immunity by a CB2 receptor-mediated, cytokine-dependent pathway. J Immunol 2000;165:373–380.
31. Smith SR, Terminelli C, and Denhardt G: Effects of cannabinoid receptor agonist and antagonist ligands on production of inflammatory cytokines and anti-inflammatory interleukin-10 in endotoxemic mice. J Pharmacol Exp Ther 2000;293:136–150.
32. Smith SR, Terminelli C, and Denhardt G: Modulation of cytokine responses in Corynebacterium parvum-primed

endotoxemic mice by centrally administered cannabinoid ligands. Eur J Pharmacol 2001;425:73–83.
33. Ouyang W, Ranganath SH, Weindel K, *et al.:* Inhibition of Th1 development mediated by GATA-3 through an IL-4-independent mechanism. Immunity 1998;9:745–755.
34. Yuan M, Kiertscher SM, Cheng Q, Zoumalan R, Tashkin DP, and Roth MD: Delta 9-tetrahydrocannabinol regulates Th1/Th2 cytokine balance in activated human T cells. J Neuroimmunol 2002;133:124–131.
35. Klein TW, Newton C, Larsen K, *et al.:* The cannabinoid system and immune modulation. J Leukoc Biol 2003;74: 486–496.
36. Klein TW, Newton C, Larsen K, *et al.:* Cannabinoid receptors and T helper cells. J Neuroimmunol 2004;147: 91–94.
37. Cecchinato V and Franchini G: Th17 cells in pathogenic simian immunodeficiency virus infection of macaques. Curr Opin HIV AIDS 2010;5(2):141–145.
38. Vinuesa CG: HIV and T follicular helper cells: A dangerous relationship. J Clin Invest 2012;122:3059–3062.
39. Montaner LJ, Doyle AG, Collin M, *et al.:* Interleukin 13 inhibits human immunodeficiency virus type 1 production in primary blood-derived human macrophages in vitro. J Exp Med 1993;178:743–747.
40. Storr M, Emmerdinger D, Diegelmann J, *et al.:* The role of fatty acid hydrolase gene variants in inflammatory bowel disease. Aliment Pharmacol Ther 2009;29:542–551.
41. Cecchinato V, Trindade CJ, Laurence A, *et al.:* Altered balance between Th17 and Th1 cells at mucosal sites predicts AIDS progression in simian immunodeficiency virus-infected macaques. Mucosal Immunol 2008;1:279–288.
42. Hartigan-O'Connor DJ, Hirao LA, McCune JM, and Dandekar S: Th17 cells and regulatory T cells in elite control over HIV and SIV. Curr Opin HIV AIDS 2011;6:221–227.
43. Hirao LA, Hokey DA, Morrow MP, Jure-Kunkel MN, and Weiner DB: Immune modulation through 4-1BB enhances SIV vaccine protection in non-human primates against SIVmac251 challenge. PLoS One 2011;6:e24250.
44. Xu H, Wang X, Liu DX, Moroney-Rasmussen T, Lackner AA, and Veazey RS: IL-17-producing innate lymphoid cells are restricted to mucosal tissues and are depleted in SIV-infected macaques. Mucosal Immunol 201;5:658–669.
45. De Filippis D, Esposito G, Cirillo C, *et al.:* Cannabidiol reduces intestinal inflammation through the control of neuroimmune axis. PLoS One 2011;6:e28159.
46. Brenchley JM, Price DA, Schacker TW, *et al.:* Microbial translocation is a cause of systemic immune activation in chronic HIV infection. Nat Med 2006;12:1365–1371.
47. Zoppi S, Madrigal JL, Perez-Nievas BG, *et al.:* Endogenous cannabinoid system regulates intestinal barrier function in vivo through cannabinoid type 1 receptor activation. Am J Physiol Gastrointest Liver Physiol 2012;302: G565–G571.
48. Ramirez SH, Hasko J, Skuba A, *et al.:* Activation of cannabinoid receptor 2 attenuates leukocyte-endothelial cell interactions and blood-brain barrier dysfunction under inflammatory conditions. J Neurosci 2012;32:4004–4016.

Address correspondence to:
Patricia E. Molina
Department of Physiology
LSUHSC
1901 Perdido Street
Medical Education Building
New Orleans, Louisiana 70112

E-mail: pmolin@lsuhsc.edu